Supplementary information

Tailoring Iron Phosphate Precursors *via* Microcrystallization for High-Performance Lithium Iron Phosphate Cathodes in Lithium-ion Batteries

Taeho Jeong,[1] Sangram Keshari Mohanty,[1] Woo Jeong Kwon,[1] Sri Charan Reddy,[1]

Aditya Ranjan Pati,[1] Ji Heon Ryu,[2] Hyun Deog Yoo[1,*]

[1] Department of Chemistry and Institute for Future Earth, Pusan National University, Busan 46241, Republic of Korea.

[2] Graduate School of Convergence Technology and Energy, Tech University of Korea, Siheung 15073, Republic of Korea.

[*]**Corresponding author:** hyundeog.yoo@pusan.ac.kr

Table S1. Particle size analysis of amorphous and various precursors materials synthesized at varying pH values

	Mean (μm)	Median (μm)	Span (μm)
A-FP	4.3	3.2	1.56
2.1-FP	2.3	2.0	1.11
2.6-FP	1.9	1.8	1.10
3.0-FP	2.0	1.9	1.13

Table S2. Observed Raman bands for $FePO_4 \cdot 2H_2O$, detailing various vibrational modes and their corresponding Raman shifts

Vibrational mode	Raman shift (cm^{-1})
Trans Fe	128.2
Trans Fe + PO_4^{3-}	199.3
Fe−O	298.2
Symmetric bend PO_4^{3-} (ν_2)	444.6
Asymmetric bend PO_4^{3-} (ν_4)	571.2
Symmetric stretch PO_4^{3-} (ν_1)	985.7
Asymmetric stretch PO_4^{3-} (ν_3)	995.8, 1031.1

Table S3. Particle size analysis of A-, 2.1-, 2.6-, and 3.0-LFP

	Mean (μm)	Median (μm)	Span (μm)
A-LFP	13.7	12.1	1.5
2.1-LFP	10.4	8.5	1.8
2.6-LFP	10.8	8.6	1.9
3.0-LFP	12.1	9.7	1.5

Table S4. Parameters obtained by fitting the impedance data using the TLM-PCD model

	pre-cycle	post-cycle
C_{tot} [mF]	4.28±0.12	9.58±0.08
σ	1.19±0.08	0.70±0.13
α_O^* [$s^{-0.5}$]	0.56±0.02	0.331±0.004
R_{ohm} [Ω]	11.57±0.03	5.25±0.02
R_{ct} [Ω]	272.2±1.7	65.7±0.2
S	0.018	0.038
χ^2	1.5×10^{-4}	2.8×10^{-4}

R_{ohm}: ohmic resistance; S: weighted sum of squares; χ^2: chi-square goodness of fit

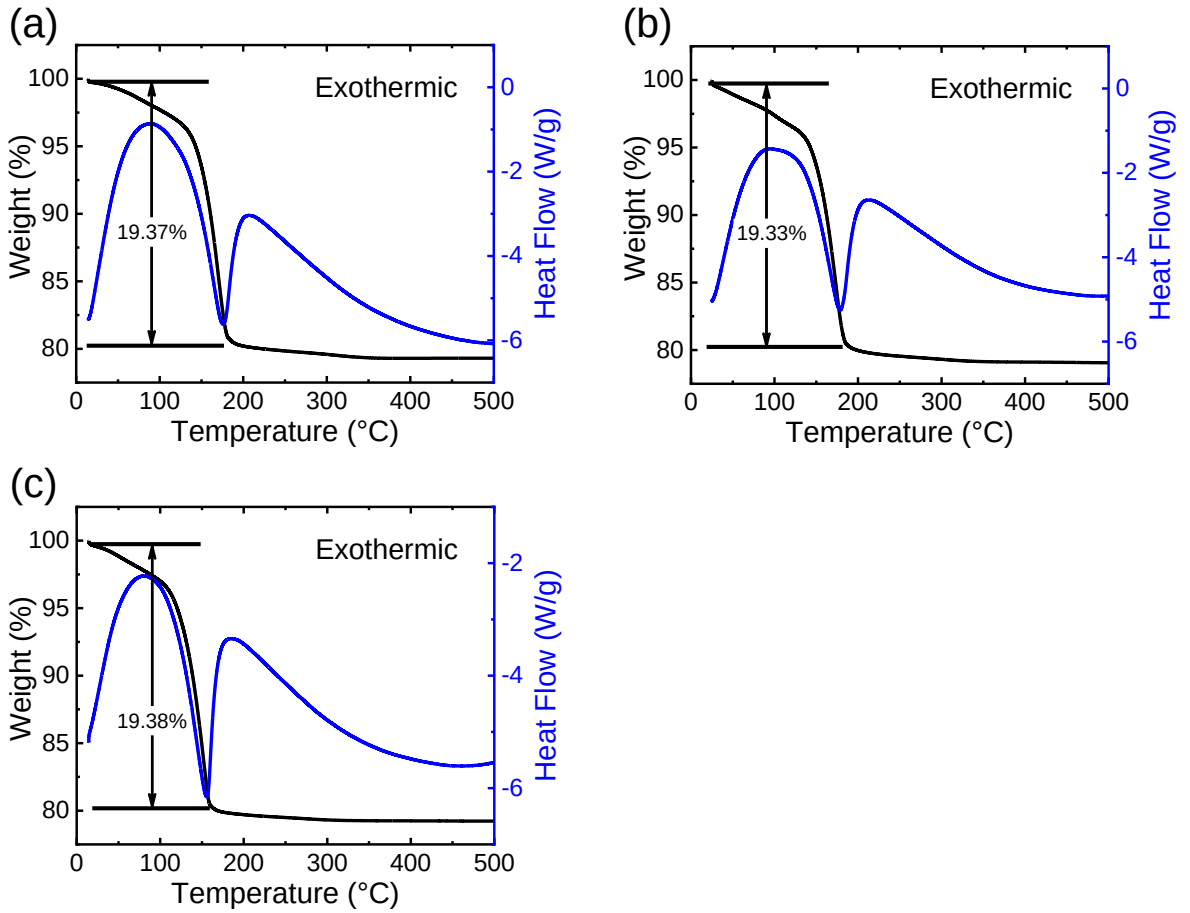

Figure S1. TGA/DSC thermograms of crystalline $FePO_4 \cdot 2H_2O$ samples synthesized at varying pH values: (a) 2.1 (b) 2.6, and (c) 3.0. Measurements were conducted in an N_2 atmosphere with a heating rate of 10 ℃/min.

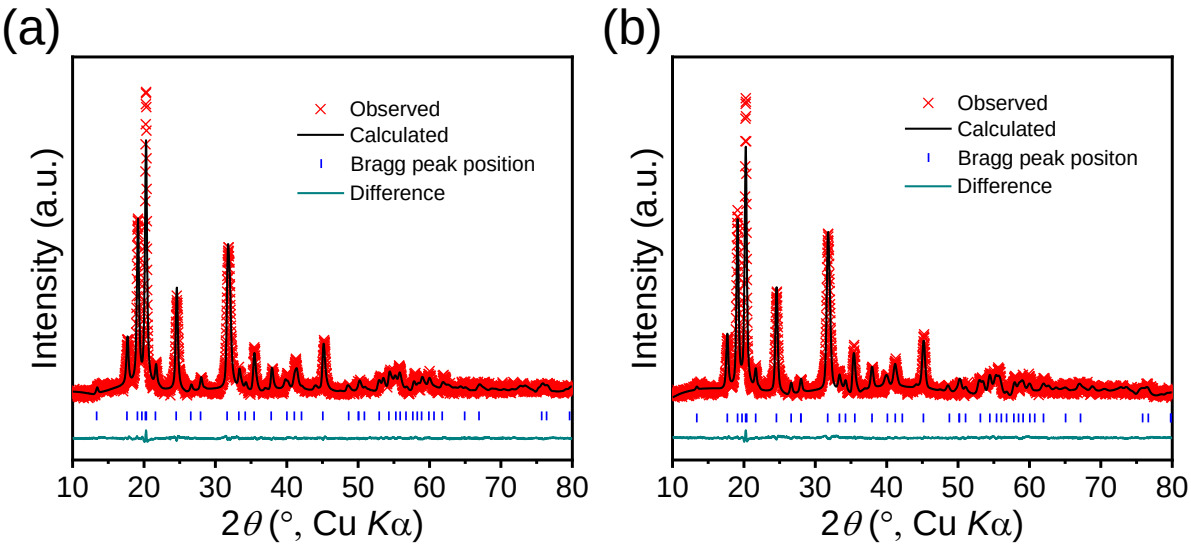

Figure S2. Rietveld refinement results for (a) 2.1-FP and (b) 3.0-FP samples.

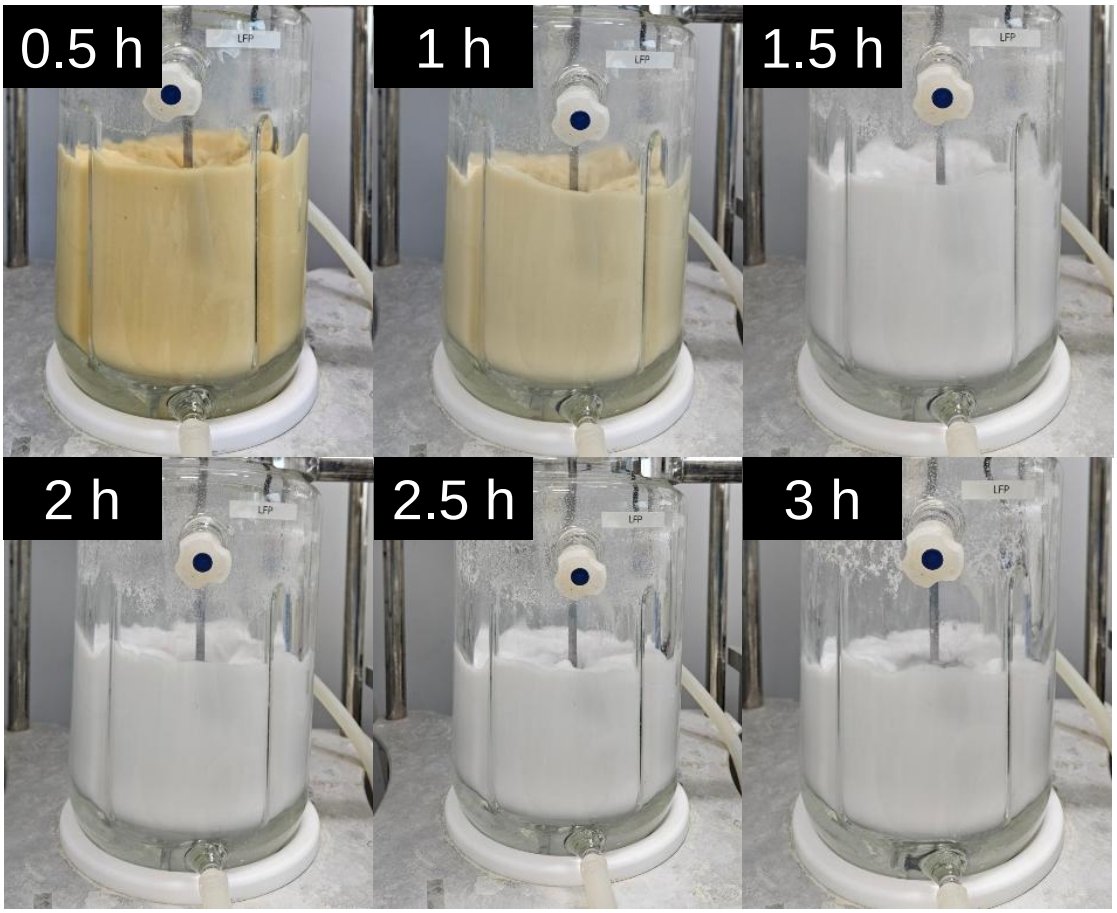

Figure S3. Color changes during microcrystallization under pH 2.6 over different time intervals: 0.5 h, 1h, 1.5 h, 2 h, 2.5 h, and 3 h.

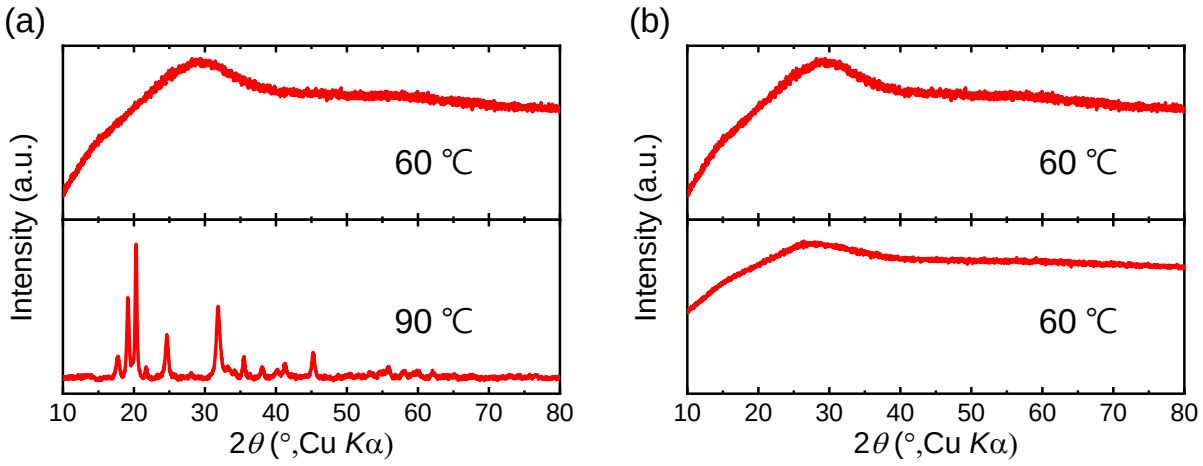

Figure S4. XRD patterns of iron phosphate precursors obtained by initial precipitation at 60 °C followed by microcrystallization at pH 2.6 and varied temperature. The upper patterns correspond to the as-precipitated amorphous precursors, while the lower patterns represent the precursors after microcrystallization at (a) 90 °C and (b) 60 °C, corresponding to crystalline $FePO_4 \cdot 2H_2O$ and amorphous $FePO_4 \cdot xH_2O$, respectively.

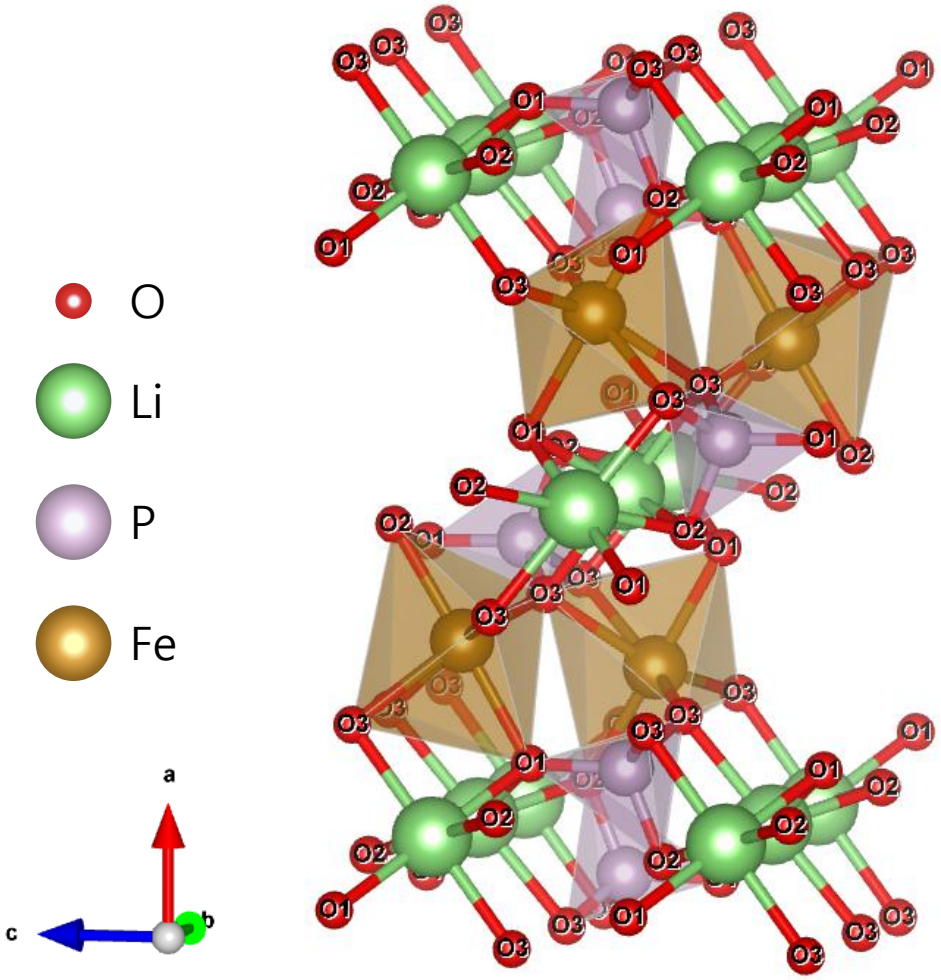

Figure S5. Polyhedral representation of the olivine structure of LFP (space group *P*nma). Brown corresponds to FeO_6 octahedra and purple corresponds to PO_4 tetrahedra. Lithium and oxygen sites are colored in green and red, respectively.

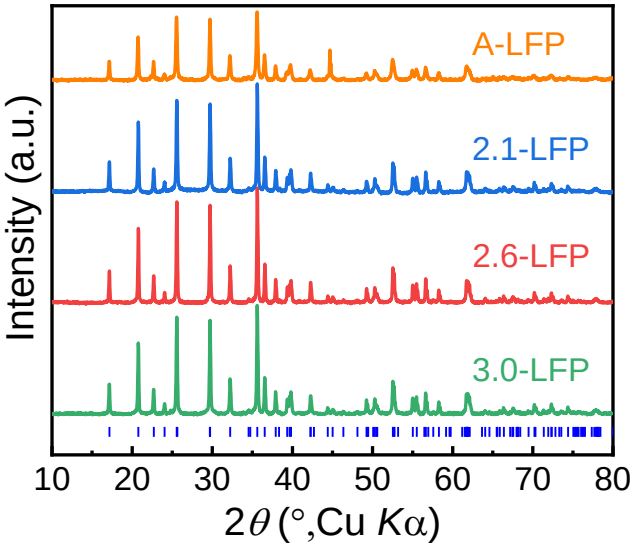

Figure S6. XRD patterns for the A-, 2.1-, 2.6-, and 3.0-LFP samples.

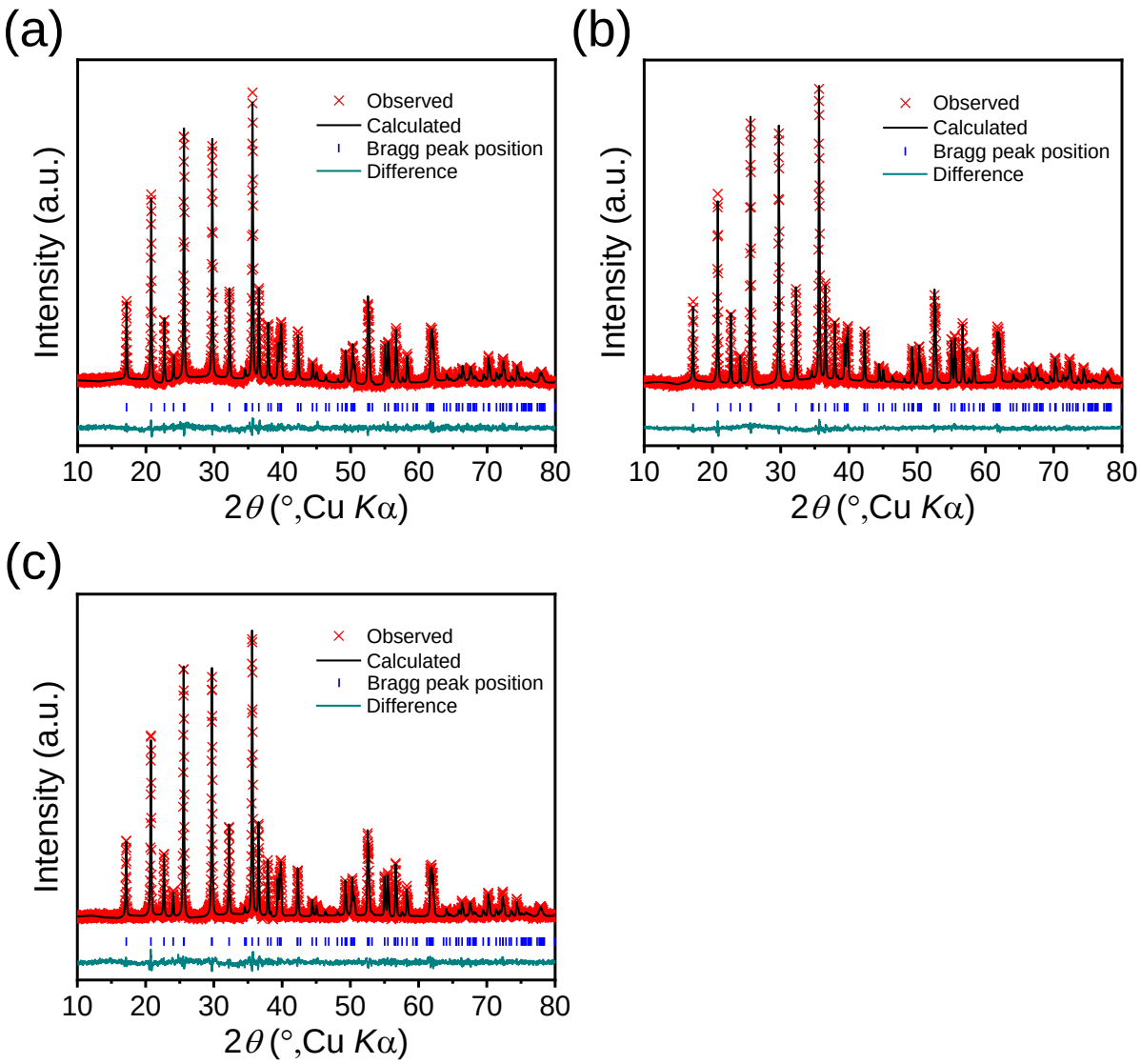

Figure S7. Rietveld refinement results for the (a) 2.1-, (b) 2.6-, and (c) 3.0-LFP samples.

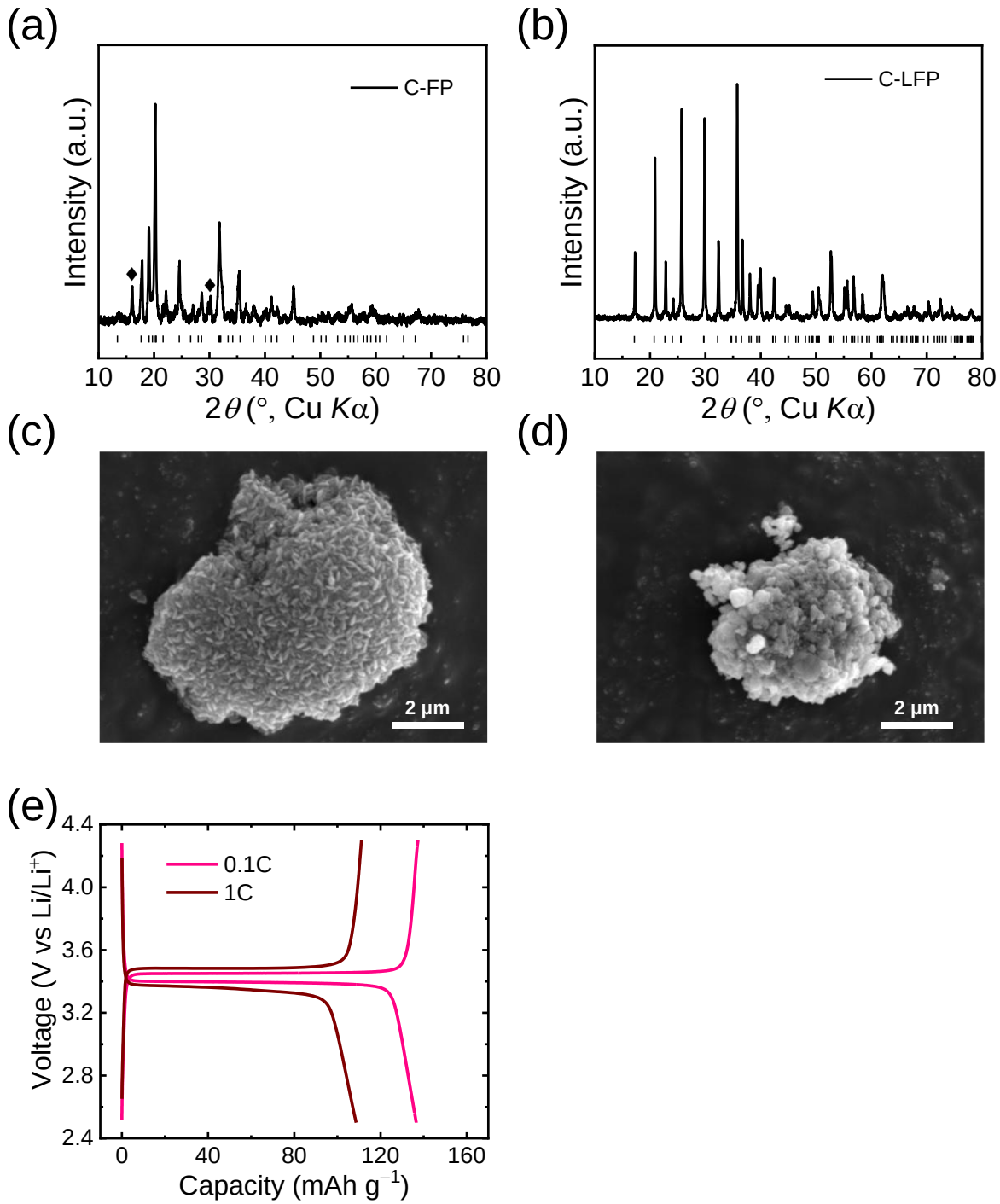

Figure S8. Characterization of commercial $FePO_4 \cdot 2H_2O$ (C-FP) and control $LiFePO_4$ (C-LFP) synthesized from C-FP: XRD patterns of (a) C-FP (space groups: $P12_1/n1$ with minor *Pbca* (◆) phases) and C-LFP (space group: *Pnma*); SEM images of (b) C-FP and (c) C-LFP, and (d) voltage profiles of C-LFP at 0.1C and 1C.

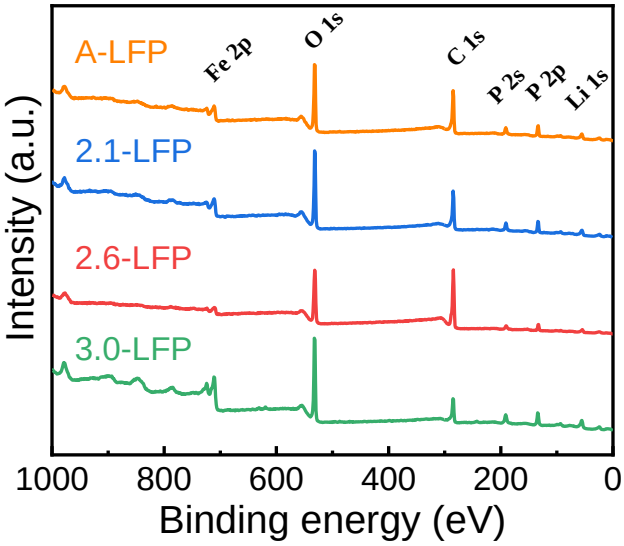

Figure S9. XPS analyses showing the survey scan of all LFP samples.

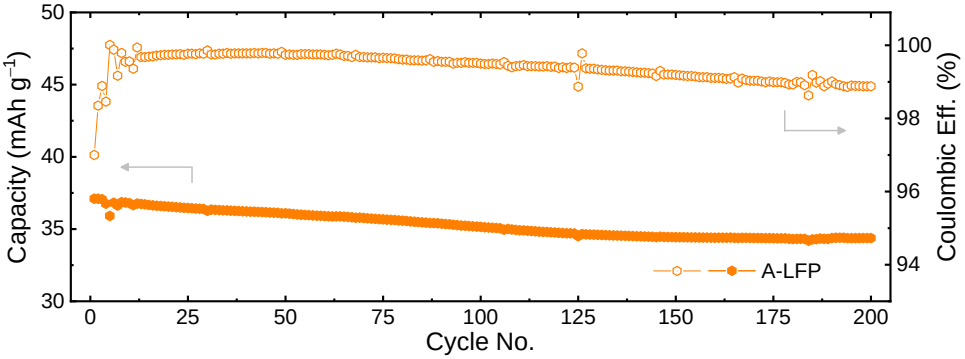

Figure S10. Cycling stability of the A-LFP sample at 1C in a half-cell.

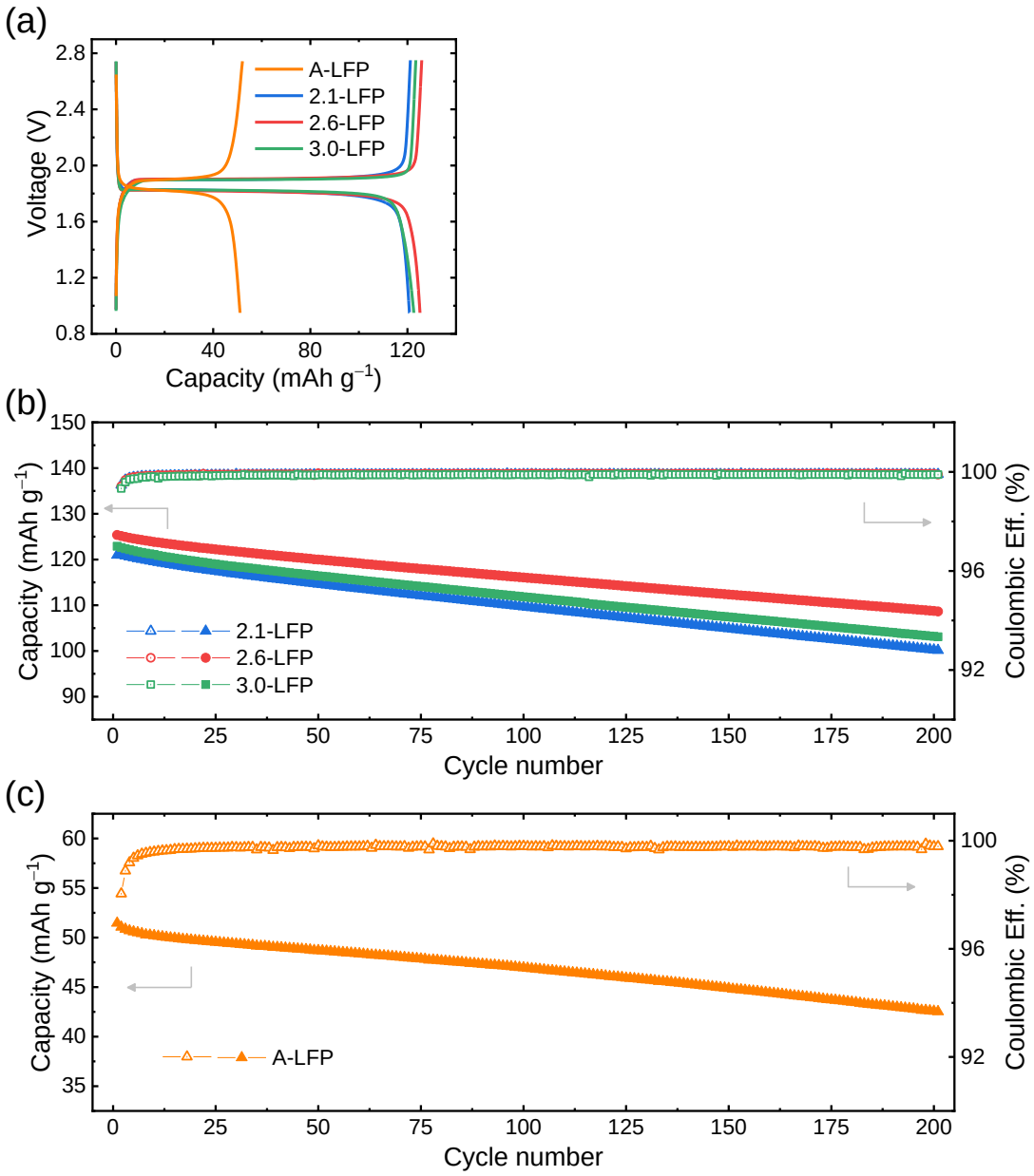

Figure S11. Electrochemical performances of the LFP | LTO full-cells: (a) voltage profiles at 1C and the cycling stability of (b) *x*-LFP | LTO cells and (c) A-LFP | LTO cell at 1C for 200 cycles within a voltage window of 0.95-2.75 V. Here, LTO stands for $Li_4Ti_5O_{12}$ anode.

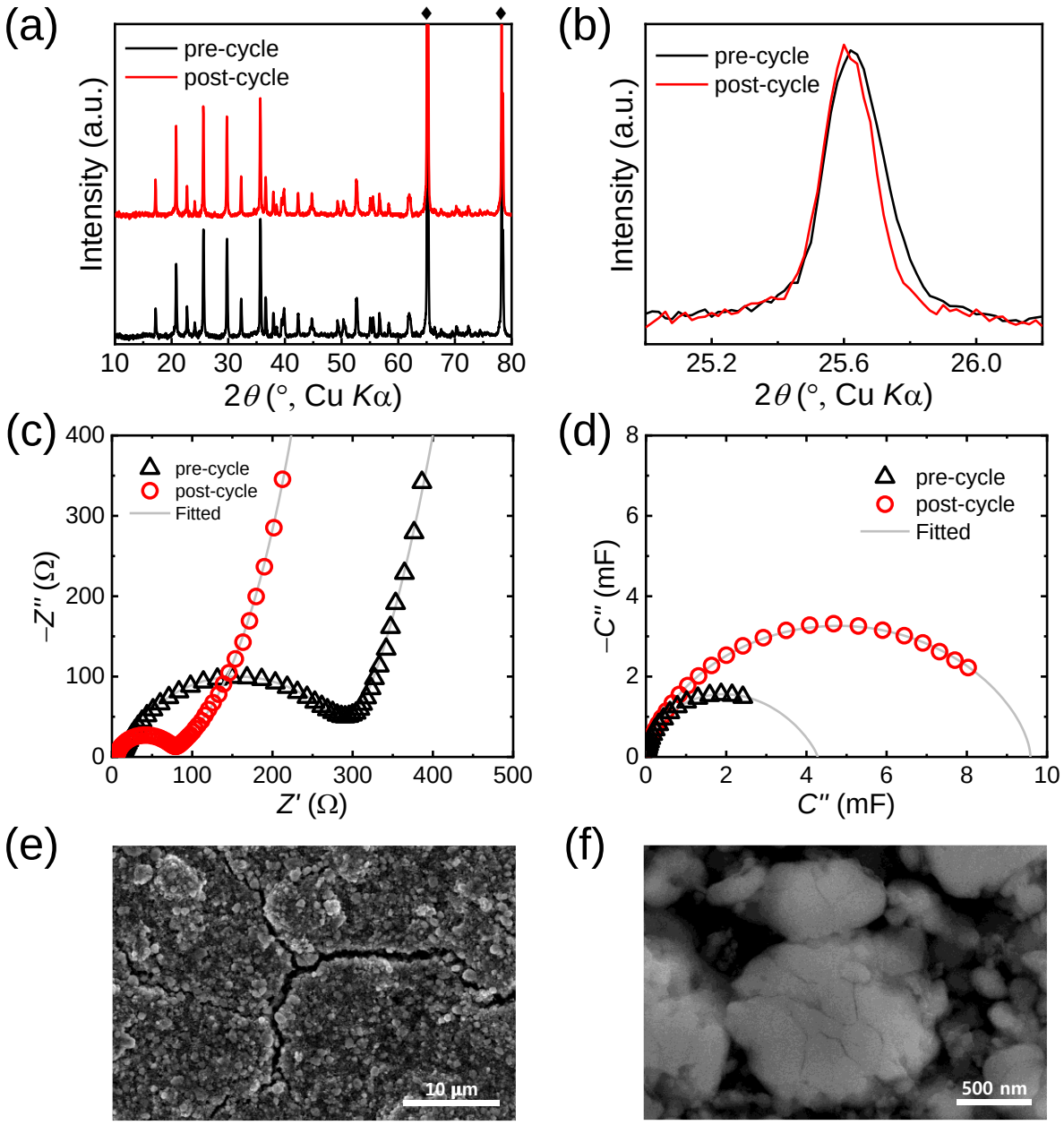

Figure S12. Post-mortem analysis of 2.6-LFP: (a, b) the XRD patterns (◆ indicates peaks for aluminum substrate), (c) the Nyquist plots and (d) the Cole-Cole plots of pre- and post-cycle impedance data (300 cycles at 1C). FE-SEM images of the electrode after 300 cycles for (e) the surface and (f) the cross-section.